IMPACT OF NEGATIVE TRIANGULARITY PLASMA SHAPING ON THE N=0 RESISTIVE WALL MODE IN A TOKAMAK

Junhyuk Song
Hanyang university, Nuclear engineering department, Seoul, South Korea

Hyojong Lee
Hanyang university, Nuclear engineering department, Seoul, South Korea

Jeffery Freidberg
MIT Plasma Science and Fusion Center, Cambridge MA 02139 United States of America

Jungpyo Lee
Hanyang university, Nuclear engineering department, Seoul, South Korea
Email: jungpyo@hanyang.ac.kr

Abstract

The axisymmetric (n=0) resistive wall mode instability is numerically investigated using a MHD instability code AVSTAB (Axisymmetric Vertical STABility) for the negative triangularity plasma shape, which has shown several benefits in terms of improved confinement time and fusion engineering. The plasma characteristics (poloidal beta and internal inductances) as well as the geometric effects (wall shape and plasma location) are important to determine the instability. In contrast to positive triangularity, the higher poloidal beta provides more instability drive for the negative triangularity because of the higher Shafranov shift and the higher elongation of the inner flux surface of the MHD equilibrium. Non-conformal wall shapes to the plasmas (positive triangularity wall and negative triangularity plasma) are found to be rather helpful to stabilize the n=0 mode, unless the plasma is too close to the walls at the nulls for the opposite triangularity.

1. INTRODUCTION

Recent experiments with a negative triangularity plasma poloidal cross section ($\delta < 0$) in the TCV and DIIID tokamaks [1-4] have revealed several unexpected benefits in terms of both plasma physics and fusion engineering. The experiments show promising performances by increasing the energy confinement time and plasma beta [3,4]. Several theoretical studies [5-8] have shown that the negative triangularity can stabilize the localized Mercier/Ballooning modes [7] with a large amount of bootstrap current [8] and reduces the electron turbulent heat flux [2,6]. In recent DIII-D negative triangularity experiments (with $\delta \simeq -0.4$) [3,4], the elongation of the plasma shape ($\kappa \simeq 1.3$) was relatively smaller than the conventional values ($\kappa \simeq 1.7$) of the positive. Increasing the elongation is highly desirable since higher elongation would result in the increase of energy confinement time $\tau_E \propto \kappa^{0.7}$[9-11]. However, besides the engineering limitation by the coils and wall, the elongation is also limited by the axisymmetric (n=0) resistive wall mode (RWM) [12-17].

To evaluate the resistive wall mode with a negative triangularity plasma in a certain wall shape, we have modified a numerical code AVSTAB (Axisymmetric Vertical STABility) [18-20]. In the code, the maximum allowable elongation (κ_{max}), in which the RWM is marginally stable, is calculated in the given feedback capability parameter $\gamma\tau_w$ [18]. The feedback parameter represents how fast instability is controllable in a given machine environment (e.g. the vacuum chamber, feedback coil positions, response time and currents). Here, γ is the instability growth rate and τ_w is the wall diffusion time. This paper more focuses on the n=0 mode through comprehensive analysis of many plasma and machine parameter. In the previous studies using AVSTAB, for convenience the plasma shape parameters were investigated only with a conformal wall shape, of which elongation and triangularity are similar to those of plasmas. It is found that the negative plasma triangularities destabilize the n=0 modes more. However, the instability significantly depends on the plasma parameters of the plasma and the wall shape.

The rest of this paper is organized as follows. In Sec. 2, we explain the characteristics of the MHD equilibrium for the negative triangular plasma shape. Shafranov shifts and the elongation are investigated using a MHD equilibrium code ECOM [21]. In Sec. 3, the effect of the plasma profiles in terms of the poloidal beta and the internal inductance on the n=0 RWM mode is investigated using AVSTAB based on the analysis of the equilibrium in Sec 2. To focus on the investigation on the plasma profile effects, we make the wall shape conformal to the plasma shape in Sec. 3. In Sec. 4, the effects of the non-conformal wall shape and the relative distance and positions of the plasma to the wall are investigated using AVSTAB. Finally, in Sec. 5, we make some conclusions of this study.

2. MHD EQUILIBRIUM OF NEGATIVE TRIANGULAR PLASMA SHAPE

To find how the MHD equilibrium of the negative triangularity plasma shape affects the n=0 RWM mode instability, the relevant characteristics of the MHD equilibrium [24,25] such as Shafranov shift and elongation are investigated in Sec. 2.1 and 2.2, respectively. Through this section, we can conclude that the negative triangularity plasma has a bigger Shafranov shift and elongations of internal flux surfaces, which will be likely connected to the larger instability of the n=0 RWM mode in Sec 3.

2.1. Shafranov shift

As shown in [20], the Shafranov shift plays an important role to find the optimal triagnualrity for the maximum elongation against the n=0 RWM mode. Using the MHD equilibrium code ECOM [21], we show in Figure 1-(a) that the negative triangular plasma shape (red curve) results in a larger shift of magnetic axis (Shafranov shift) compared to the positive triangularity shape (blue curve). The simulation uses the DIIID parameters of [3] ($R_0 = 1.7m, \kappa = 1.3, a = 0.59m, I_p = 0.9MA, B_t = 2.0T$) with different triangularities. The change of the magnetic axis is numerically examined by adjusting the radial pressure profiles for the desired poloidal beta and internal inductance as done in [20] (e.g. pressure gradient is adjusted by $dp/d\Psi = p_0\left(1-\hat{\Psi}^2\right)^{pout}$). Here, the normalized radius is defined as the normalized poloidal flux $r/a \equiv \hat{\Psi} \equiv (\Psi - \Psi_0)/(\Psi_{LCFS} - \Psi_0)$, where Ψ, Ψ_0 and Ψ_{LCFS} are the poloidal flux at a flux surface, the magnetic axis, and the last closed flux surface. Fig 1-(b) shows that the normalized Shafranov shift (Δ/a) almost proportionally increases by the summation of the poloidal beta and a half of the internal inductance, as proven analytically in the large aspect ratio [22,23]. Here, Δ is the shift of the magnetic axis toward the low field side, and a is the minor radius. While the linear slope gradient does not change much with triangularity, the y intercept increases significantly as the triangularity decreases.

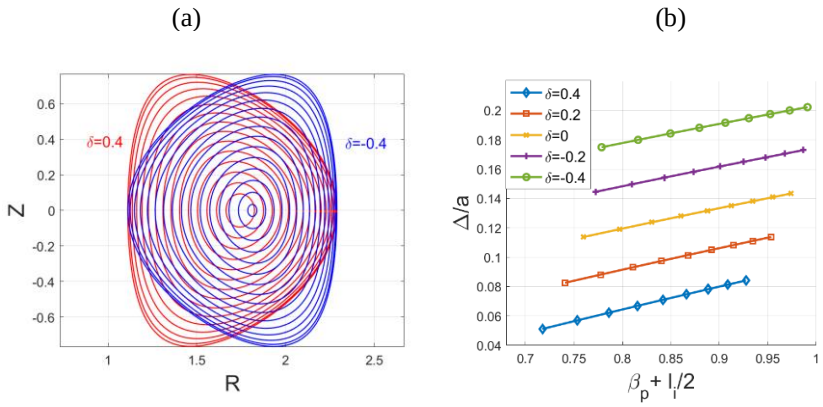

Fig. 1. (a) Contour plots of poloidal magnetic fluxes for two MHD equilibria with different triangularities ($\delta = -0.4$ and $\delta = +0.4$), and (b) normalized Shafranov shift in terms of the summation of poloidal beta and a half of internal inductance $\beta_p + l_i/2$ for many triangularities simulated by ECOM.

This relation between the triangularity and the Shafranov shift can be explained by examining the iso-surface boundary condition of the Grad-Shafranov equation in the last-closed flux surface. Based on the following Miller geometry parametrization [26] for the last-closed flux surface

$$R = R_0 + a\cos(\theta + sin^{-1}(\delta)\,sin\,\theta)$$

$$Z = Z_0 + \kappa a \sin\theta, \qquad (1)$$

The distance from the magnetic axis in the last-closed flux surface is

$$r_a(\theta) = a\sqrt{(\cos^2(\theta + \sin^{-1}\theta\,\sin\theta) + \kappa^2\sin^2\theta)}, \qquad (2)$$

and for $\kappa = 1.0$ and a small δ it satisfies approximately

$$\frac{r_a(\theta)}{a} \simeq 1 - \delta \sin^2\theta \cos\theta \equiv \sum_m \hat{r}_m \cos(m\theta),$$

where the last equation is the Fourier series for the up-down symmetric tokamak.

The Shafranov shift is determined by the first poloidal Fourier mode of the Grad-Shafranov equation solution in the first order of $\epsilon = r/R_0$ [23]. The first poloidal mode of the poloidal magnetic flux $\Psi_{m=1}$ is affected by the boundary condition change due to the triangularity $\hat{r}_{m=1} \simeq -\delta/4$, and it results in the approximate relation of the Shafranov shift change by the triangularity $\Delta(\delta) - \Delta(\delta = 0) \propto -\delta a$, as shown in Fig. 1-(b).

2.2. Elongation of inner flux surfaces

The elongated plasma shape is susceptible to be unstable for the vertical instability by the n=0 RWM mode, so it is important to find how much the inner flux surfaces as well as the last-closed flux surface are elongated for the different triangularity in the MHD equilibrium.

The Miller elongation parameter of each flux surface $\kappa(r)$ can be estimated by the nonlinear regression of MHD equilibrium using ECOM with the fixed elongation of the last closed flux surface ($\kappa(r = a) = 1.7$) of Eq.(1). It is found that the negative and positive triangularites have significantly different radial profiles of the elongations in terms of radius. While the positive triagnualrity ($\delta = 0.4$) shows the monotonically decrease of the elongation toward the center as expected, the negative triangulariy ($\delta = -0.4$) shows somewhat increases of the elongation below a specific radius ($r/a \sim 0.6$) and results in much higher elongation at the center $\kappa(r = 0)$ than the positive triangularity.

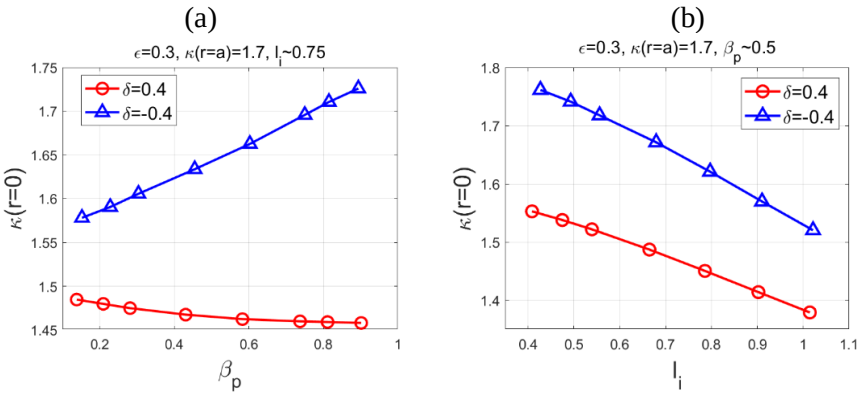

Fig. 2. (a) Elongation at the plasma center $\kappa(r = 0)$ for the fixed last closed flux surface elongation $\kappa(r = a) = 1.7$ in terms of poloidal beta β_p with $a/R_0 = 0.3$ and $l_i \simeq 0.75$ (b) Elongation at the plasma center $\kappa(r = 0)$ for the fixed last closed flux surface elongation $\kappa(r = a) = 1.7$ in terms of internal inductance l_i with $a/R_0 = 0.3$ and $\beta_p \simeq 0.5$

Fig. 2 shows the change of the elongation at the plasma center ($\kappa(r = 0)$) in the same fixed elongation of the last closed flux surface ($\kappa(r = a) = 1.7$) by varying the poloidal beta and the internal inductance for different triangularites. The effects of poloidal beta in Fig. 2-(a) are significantly different between the negative and the positive triangularities. While the elongation at the center for the negative triangularity increases almost proportionally to the poloidal beta, that for the positive triangularity does not change much and even decreases somewhat. Fig. 2-(b) shows that the elongation at the center increases as the internal inductance decreases for both triangularites, but the negative triangularity has a larger elongation at the center than the positive triangularity for all range of internal inductance.

The effect of the poloidal beta on the elongation in Fig. 2-(a) and the effect on the Shafranov shift in Figure 1-(b) are likely correlated in the solution of the Grad-Shafranov equations for the MHD equilibrium. However, it is worth noting for the negative triangularity that both effects make the impact on the instability in the same direction,

in which of the high poloidal beta makes the plasmas more unstable to the n=0 RWM, as will be more explained in Section 3.

3. N=0 RESISTIVE WALL MODE OF NEGATIVE TRIANGULAR PLASMA SHAPE

The negative triangular plasma shape is likely more unstable for the n=0 RWM mode in the conformal wall shape. In this section, we study the main characteristics of the plasma profile dependency in terms of the poloidal beta and the internal inductance on the instability for the negative triangularity.

From the energy principle with a thin wall limit in [18,19], the Lagrangian integral δW is expressed as follows,

$$\delta W_{total} = \delta W_F + \delta W_{VI} + \delta W_{VO} + \alpha W_D \quad (3)$$

where the fluid contribution in the plasma region is

$$\delta W_F = \frac{1}{2\mu_0}\int_{V_P}\left[\frac{(\nabla\psi)^2}{R^2} - \left(\mu_0 p'' + \frac{1}{R^2}F''^2\right)\psi^2\right] d\vec{r} + \frac{1}{2\mu_0}\int_{S_P}\left(\frac{\mu_0 J_\phi}{R^2 B_P}\psi^2\right) dS, \quad (4)$$

the inner vacuum contribution is

$$\delta W_{VI} = \frac{1}{2\mu_0}\int_{VI}\frac{\left(\nabla\hat{\psi}\right)^2}{R^2} d\vec{r}, \quad (5)$$

the wall contribution is

$$W_D = \frac{1}{2\mu_0}\int_{SW}\frac{\hat{\psi}^2}{R^2} dS. \quad (6)$$

and the outer vacuum contribution is

$$\delta W_{VO} = \frac{1}{2\mu_0}\int_{VO}\frac{\left(\nabla\hat{\hat{\psi}}\right)^2}{R^2} d\vec{r}, \quad (7)$$

Here, ψ, $\hat{\psi}$, $\hat{\hat{\psi}}$ are the perturbed poloidal fluxes due to the RWM in the plasma region, in the inner vacuum region, and in the outer vacuum region, respectively, $\alpha = \gamma\mu_0\sigma d$, μ_0 is the vacuum permeability, σ the wall conductivity and d the thickness of the wall, as following the notation in [18,19]. The negative δW indicates the unstable n=0 RWM mode in a given feedback parameter $\gamma\tau_w \simeq \alpha b$, where b is the effective radius of the wall by $b \sim L_w/2\pi$.

3.1. Poloidal beta (β_p) dependency

The impact of the poloidal beta on the n=0 RWM instability is well correlated to the impact of the poloidal beta on the MHD equilibrium shown in Section 2. In the previous studies [19,20], it was found in the conformal wall that the optimal triangularity, in which the instability is minimized and the allowable elongation is maximized, increases as the inverse aspect ratio ($\epsilon = a/R_0$) increases and the poloidal beta increases. It is shown in Figure 3 of [19], and the fitting formula $\delta_{opt} \propto \epsilon^{-1.22\beta_p}$ in [20]. Fig. 3-(a) also shows the same trends but provides more information with the negative triangular shape. As the poloidal beta increases, the maximum allowable elongation in the MHD stability analysis decreases for the negative triangularity, while it increases for the positive triangularity. The different behavior in the MHD equilibrium between the negative and positive plasma shapes, is likely one of reasons of the n=0 RWM instability, because the higher Shafranov shift and the elongations of the inner flux surface are susceptible for the vertical instability.

This correlation is well represented in Fig. 3-(b) showing the plasma contribution of the inner flux surface δW_F in terms of the poloidal beta for many triangularities. The inner flux surface contribution by the different MHD equilibrium for the different triangularity has the different dependency on the poloidal beta: δW_F increase (toward stabilization) almost proportionally by the increased poloidal beta for the positive triangularities, while it is reversed for negative ones. This sensitivity on the poloidal beta becomes severe in the large absolute values of the triangularity.

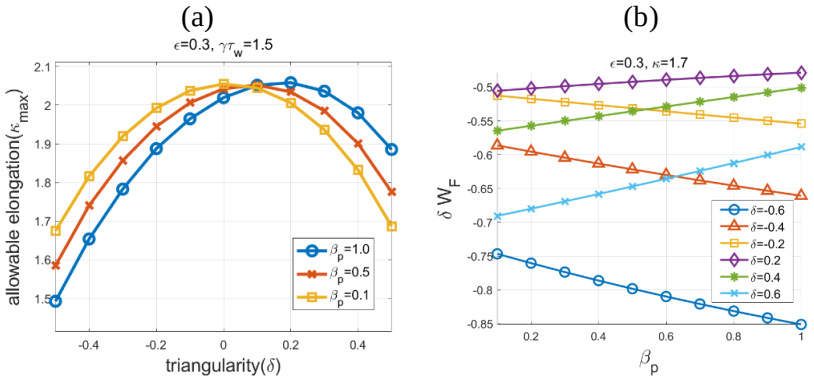

Fig. 3. (a) Maximum allowable elongation κ_{max} against the n=0 RWM in terms of triangularity with the different poloidal beta, using AVSTAB simulations for $\epsilon = a/R_0 = 0.3$, $\gamma\tau_w = 1.5$, and $\Delta_i = \Delta_o = \Delta_v/3 = 0.1$ (b) Fluid contribution in the plasma regime to the Lagrangian integral δW_F in terms of poloidal beta β_p for the different triangularities in the conformal wall with the fixed inverse aspect ratio ($\epsilon = 0.3$) and elongation ($\kappa = 1.7$).

3.2. Internal inductance (l_i) dependency

The impact of the internal inductance on the stability is dominantly determined by the effective distance between the wall and plasmas [20]. As shown in Fig. 4, the lower internal inductance is generally good for the stabilization of all triangular shapes by the shorter effective distance between the wall and plasmas. On the other hands, according to Fig. 2-(b) and 3-(b), the impacts of the Shafranov shift and the inner flux surface elongation changes by the internal inductance on the instability are more complex, but they are possibly minor factors determining the instability compared to the effective distance. The lower internal inductance is good for the stability by reducing Shafranov shift, but bad for the stability by increasing the elongations of the inner flux surface.

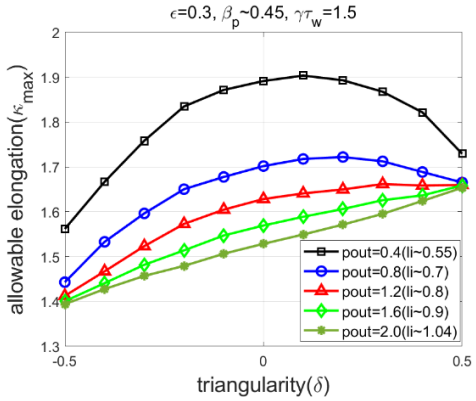

Fig. 4. Maximum allowable elongation κ_{max} against the n=0 RWM in terms of triangularity with the different internal inductance, using AVSTAB simulations for $\epsilon = a/R_0 = 0.3$, $\gamma\tau_w = 1.5$, and $\Delta_i = \Delta_o = \Delta_v/3 = 0.1$. In the plasma pressure radial profile by $dp/d\psi \sim (1-\psi^2)^{pout}$, the parameter pout in ECOM is used to adjust the different l_i

4. WALL EFFECTS ON THE N=0 RWM

Although the conformal wall condition in Section 3 is theoretically useful to analyze the plasma parameter effects, it is likely somewhat different from the real experimental conditions because the wall shape is usually static even when the different plasma shape control is available. In this section, we investigate the effects of the fixed wall shape and the relative position of the plasma to the wall on the n=0 RWM instability for different triangularities numerically using the AVSTAB code.

4.1. Non-conformal wall shape

Interestingly, the wall shape conformal to the plasma does not always minimize the n=0 instability. Figure 5-(a) shows the maximum elongation against the n=0 mode simulated in AVSTAB in terms of the plasma triangularity

for the different wall triangularities δ_w as depicted in the 2-D plots of boundaries in Fig. 5-(b). Compared to the conformal wall of the same triangularities between the wall and plasmas (black curve of $\delta_w = \delta$), the non-conformal wall by the fixed wall triangularites (red curve of $\delta_w = 0.3$ and blue curve of $\delta_w = -0.3$) are more stabilizing in the optimal plasma triangularity. For the positive wall triangularity of $\delta_w = 0.3$, the negative plasma triangularity around $\delta_w \simeq -0.3$ is optimal for the stabilization. For the negative triangularity of $\delta_w = -0.3$, the positive plasma triangularity around $\delta_w \simeq 0.3$ is optimal for the stabilization. In this case, the inner gap distance and the outer gap distance between the plasma and wall shapes in the mid-plane are fixed as $\Delta_i = \Delta_o = 0.2$, and the wall triangularity is adjusted by $\kappa_w = \kappa + 0.3$ to avoid the geometrical crossing between the plasma and wall shapes. The dashed lines of Fig. 5-(a) represent the elongation, in which the plasma shape starts to cross the wall shape. Thus, before approaching the geometric crossing, the maximum elongation is reduced as a result of the stability analysis.

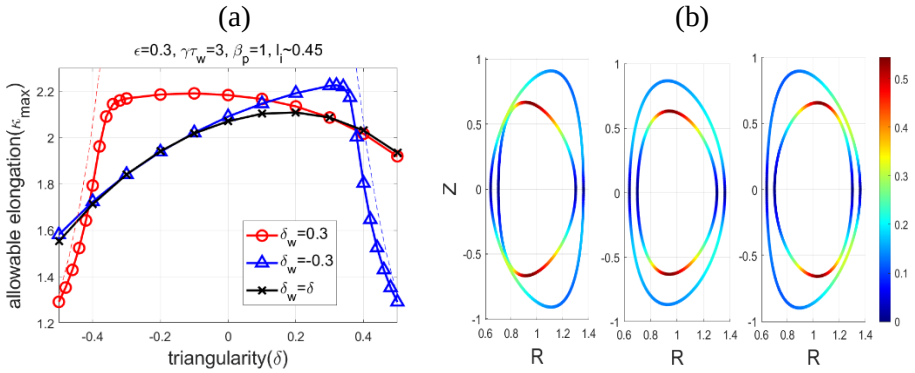

Fig. 5. (a) Maximum allowable elongation κ_{max} against the n=0 RWM in terms of plasma triangularity with different wall triangularities. The red and blue curves have the fixed wall triangularities of $\delta_w = 0.3$ and $\delta_w = -0.3$, while black curve represent the conformal wall. The constant gap is set as $\Delta_i = \Delta_o = 0.2$. The red and blue dashed lines are the boundaries when the plasma and wall shapes start crossing geometrically. (b) A color map of the perturbed poloidal magnetic flux ψ and $\hat{\psi}$ of Eqs. (4-6) on the plasma and wall boundaries in the 2-D (R, Z) coordinates for the optimal plasma triangularities of three wall cases in (a).

Figure 6 shows two-dimensional contour plots of the maximum elongation against n=0 mode in terms of the plasma triangularity and the wall triangualrity. The conformal wall ($\delta_w = \delta$) corresponds to the diagonal lines (dashed lines) of the planes. The optimal conditions of the plasma and wall triangularities are clearly shown in the two peaks (yellow contours), which are apart from the diagonal lines. For the small gaps $\Delta_i = \Delta_o \leq 0.3$, there will be two forbidden areas (at the upper left and lower right corners) having a sharp drop of the maximum elongation as the degree of the non-conformality between the wall and plasma triangularity becomes more severe. It is because that even the intermediate level of the elongation of plasmas can have a tiny distance between the wall and plasmas just before the plasmas are crossing the walls geometrically. This adjustment of the maximum elongation due to the geometrical crossing is more clearly shown in the next subsection, in which the different plasma locations in the mid-plane are simulated in the non-conformal walls.

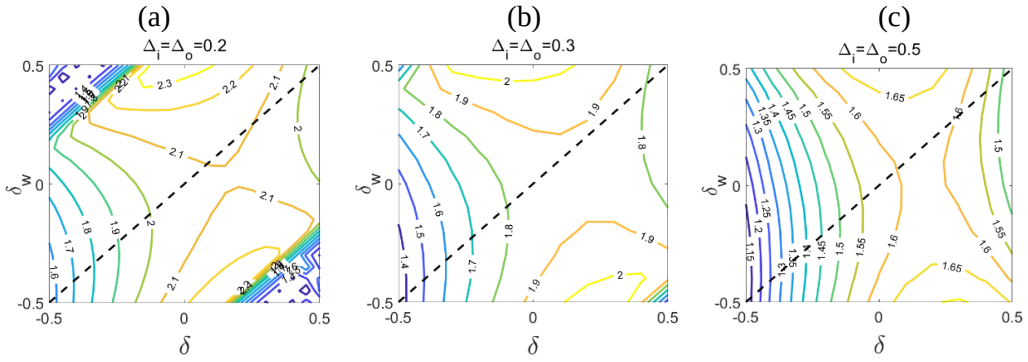

Fig. 6. Contour plots of the maximum allowable elongation κ_{max} against the n=0 RWM in two dimensions of the plasma and the wall triangularities (δ, δ_w) for three different gap distances between plasma and wall: (a) $\Delta_i = \Delta_o = 0.2$, (b) $\Delta_i = \Delta_o = 0.3$, and (c) $\Delta_i = \Delta_o = 0.5$.

4.2. Plasma location change in the mid-plane

Plasma center location in the mid-plane relative to the wall is also an important parameter to determine the instability. Figure 7 shows the change of the maximum elongation against the n=0 mode by the plasma center position R_0. Here R_0 is not the magnetic axis of the MHD equilibrium but the center of major radius for the last-closed flux surface given in Eq. (1). Hence R_0 does not contain the Shafranov shift but it represents the change of the difference between the inner gap and the outer gap in the mid-plane with the conditions of the fixed wall and plasma aspect ratio (i.e. $R_0/R_{0w} = 1 + (\Delta_i - \Delta_o)/2$ and $\Delta_i + \Delta_o =$ constant, where R_{0w} is the wall center location). The concentric plasma and wall shapes occurs at $R_0/R_{0w} = 1$.

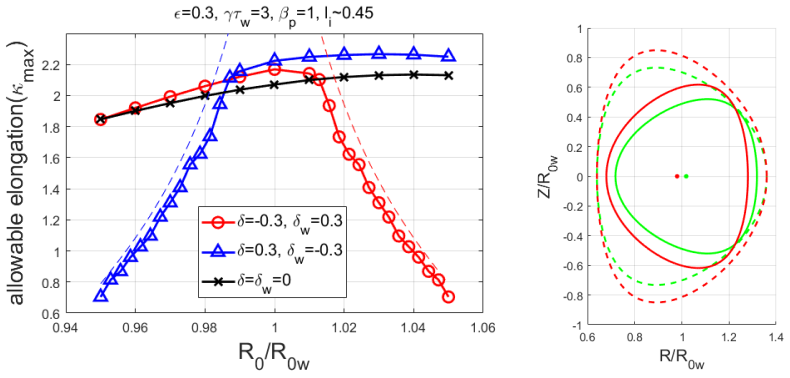

Fig. 7. (a) Maximum allowable elongation κ_{max} against the n=0 RWM in terms of major radius of the plasma center relative to the wall center (plasma location in the mid-plane) R_0/R_{0w} with $\epsilon = a/R_0 = 0.3$, $\gamma\tau_w = 3$, and $\Delta_i + \Delta_o = 0.4$ (b) The plasma (solid line) and wall (dashed line) shapes in 2-D (R_0/R_{0w}, Z/R_{0w}) coordinates for two plasma centers $R_0/R_{0w} = 0.98$ (red) and $R_0/R_{0w} = 1.02$ (green) of the case of $\delta = -0.3$ and $\delta_w = 0.3$ (red curve) in (a)

From Fig. 7-(a), we find that for both the conformal walls (black curve) and the non-conformal walls (red and blue curves), the small move of the plasma center toward the low-field side results in more stabilization. In other words, in the Miller shape, the optimal conditions maximizing the stabilization occurs when $R_0/R_{0w} \simeq 1.03$ regardless of the different plasma and wall triangularites.

However, the large move of the plasma center toward any directions can degrade the stabilization effects. For the opposite triangularity cases, the degradation occurs seriously when the distance between the plasma nulls and the wall is tiny (e.g. $R_0/R_{0w} \simeq 0.98$ for $\delta = 0.3$ and $\delta_w = -0.3$, and $R_0/R_{0w} \simeq 1.05$ for $\delta = -0.3$ and $\delta_w = 0.3$. From the δW partition analysis, a significant decrease of the vacuum contribution is observed for the sharp degradation. The significant increase of the instability also corresponds with the geometric crossing between the plasma and wall shapes. The geometric constraints of the plasma elongation, in which plasmas cannot cross with the wall, is still valid in the stability analysis.

5. CONCLUSIONS

In this paper, the characteristics of the negative triangular plasma shapes in terms of the n=0 MHD resistive wall mode instability and the MHD equilibrium are examined computationally. The plasma properties and the wall geometry are considered as the key parameters to determine the characteristics compared to the positive triangular plasma shapes. The poloidal beta of the plasmas makes the different impacts on the instability depending on the plasma shape. According to Fig 3, the higher poloidal beta provides more instability of RWM for the negative triangular plasma shape, while it provides more stabilization for the positive triangular plasma shape. This characteristic is likely derived from the higher Shafranov shift and the higher elongation of the inner flux surface of the MHD equilibrium for the negative triangular plasma shape, making more unstable fluid plasma contribution δW_F.

The non-conformal wall effects in this study are somewhat surprising. In spite of the misalignment between the plasma and wall boundaries, the different triangularity of the plasma and wall can cause more stabilizing effects in total. According to Figs. 5-8, the negative triagnular plasma shape with the positive triangular wall shape can have a higher allowable elongation against the n=0 mode compared to both positive triangular plasma and wall shapes. However, it has the optimal conditions in the degree of the difference of non-conformality. If the absolute value of the negative plasma triangularity is too large, it degrades the stabilization. It also corresponds to the dangerous conditions when the plasma is too close to the wall at the nulls for the opposite triangularity. If the gap

between the plasma and the wall is sufficiently large to avoid this crossing, the low level of the non-conformality due to the opposite triangualarity is rather helpful for the n=0 RWM stabilization. It is worth verifying the characteristics of negative triangularity shape theoretically found in this paper in some tokamak experiments near future.

ACKNOWLEDGEMENTS

This work was supported by the National Research Foundation of Korea (NRF) grant funded by the Korea government (MSIT) (NRF-2019R1F1A1058298)

REFERENCES

[1] Camenen Y., Pochelon A., Behn R., Bottino A., Bortolon A., Coda S., Karpushov A., Sauter O., Zhuang G. and the TCV team, Impact of plasma triangularity and collisionality on electron heat transport in TCV L-mode plasmas, Nucl. Fusion **47** (2007).

[2] Fontana M., Porte L., Coda S., Sauter O. and TCV Team, The effect of triangularity on fluctuations in a tokamak plasma, Nucl. Fusion **58** 024002 (2018).

[3] Austin M.E. et al., Achievement of reactor-relevant performance in negative triangularity shape in the DIII-D tokamak, Phys. Rev. Lett. **122** 115001 (2019).

[4] Austin M.E., Reactor-friendly core and boundary of DIII-D diverted negative triangularity plasmas with persistent L-mode edge, 62nd Annual Meeting of the APS Division of Plasma Physics (2020).

[5] Zheng L. J. et. al., "Negative Triangularity Effects on Tokamak MHD Stability", IAEA Fusion Energy Conference (TH/P5-31), (2018).

[6] M. Kikuchi et al., L-mode-edge negative triangularity tokamak reactor, Nucl. Fusion **59** 056017 (2019).

[7] Medvedev S.Yu. et al., The negative triangularity tokamak: stability limits and prospects as a fusion energy system, Nucl. Fusion **55** 063013 (2015).

[8] Scotti F., et al., Divertor heat flux profiles in negative triangularity DIII-D discharges, 62nd Annual Meeting of the APS Division of Plasma Physics (2020).

[9] Lomas P. J. and JET Team, The variation of confinement with elongation and triangularity in ELMly H-modes on JET, Plasma Physics and Controlled Fusion **42** B115 (2000).

[10] Kinsey J. E., et. al., The effect of plasma shaping on turbulent transport and E × B shear quenching in nonlinear gyrokinetic simulations, Phys. Plasmas **14** 102306 (2007).

[11] ITER Physics Expert Groups on Confinement and Transport and Confinement Modelling and Database, et. al., Chapter 2: Plasma confinement and transport, Nucl. Fusion **39** 2175 (1999).

[12] Laval G. and Pellat R., Controlled fusion and plasma physics, Proc. 6th Europ. Conf. (Moscow) vol 2 p 640 (1973).

[13] Wesson J.A. and Sykes A., Toroidal calculations of tokamak stability, Proc. 5th Int. Conf. (Tokyo) vol 1 p 449 (1975).

[14] Becker G. and Lackner K., Plasma physics and controlled nuclear fusion research, Proc. of the 6th Int. Conf. (Berchtesgaden)vol 2 p 401 (1977).

[15] Wesson J.A., Controlled fusion and plasma physics, Proc. 7th European Conf. (Lausanne) vol 2 p 102 (1975).

[16] Wesson J.A., Hydromagnetic stability of tokamaks Nucl. Fusion **18** 87 (1978).

[17] Lazarus E.A. et al., Higher beta at higher elongation in the DIII-D tokamak, Phys. Fluids B **3** 2220-2229 (1991).

[18] Freidberg J.P. et al., Tokamak elongation: how much is too much? Part 1. Theory, J. Plasma Phys. **81** 515810607 (2015).

[19] Lee J.P et al, Tokamak elongation: how much is too much? Part 2. Numerical results, J. Plasma Phys. **81** 51580608 (2015).

[20] Lee J.P et al., An analytic scaling relation for the maximum tokamak elongation against n = 0 MHD resistive wall modes, Nucl. Fusion **57** 066051 (2017).

[21] Lee J.P. and Cerfon A., ECOM: A fast and accurate solver for toroidal axisymmetric MHD equilibria, Comp. Phys. Comm. **190** 72 (2015).

[22] Shafranov V., Sov. Phys. JETP **6** 545 (1958).

[23] Lee J.P. and Cerfon A., Plasma Phys. Control. Fusion **61** 105007 (2019)

[24] Guazzotto L. and Freidberg J. P., Simple, General, Realistic, Robust, Analytic, Tokamak Equilibria, I. Limiter and Divertor Tokamaks, J. Plasma Phys (2021)

[25] Guazzotto L. and Freidberg J. P., Simple, General, Realistic, Robust, Analytic, Tokamak Equilibria II. Pedestals and Flow, J. Plasma Phys. (2021)

[26] Miller R.L., Chu M.S., Greene J.M., Lin-Liu Y.R., Waltz R.E., Phys. Plasmas **5** 973 (1998)